Published in final edited form as:

Biopolymers. 2019 June ; 110(6): e23277. doi:10.1002/bip.23277.

Helical side chain chemistry of a peptoid-based SP-C analogue: balancing structural rigidity and biomimicry

Nathan J. Brown[1], **Jennifer S. Lin**[2], **Annelise E. Barron**[2,*]

[1]Department of Chemical and Biological Engineering, Northwestern University, Evanston, Illinois

[2]Department of Bioengineering, Stanford University, 443 Via Ortega, Stanford, CA 94305

Abstract

Surfactant protein C (SP-C) is an important constituent of lung surfactant (LS) and, along with SP-B, is included in exogenous surfactant replacement therapies for treating respiratory distress syndrome (RDS). SP-C's biophysical activity depends upon the presence of a rigid *C*-terminal helix, of which the secondary structure is more crucial to functionality than precise side chain chemistry. SP-C is highly sequence-conserved, suggesting that the β-branched, aliphatic side chains of the helix are also important. Non-natural mimics of SP-C were created using a poly-*N*-substituted glycine, or "peptoid," backbone. The mimics included varying amounts of α-chiral, aliphatic side chains and α-chiral, aromatic side chains in the helical region, imparting either structural rigidity or biomimicry. Biophysical studies confirmed that the peptoids mimicked SP-C's secondary structure and replicated many of its surface-active characteristics. Surface activity was optimized by incorporating both structurally rigid and biomimetic side chain chemistries in the helical region indicating that both characteristics are important for activity. By balancing these features in one mimic, a novel analogue was created that emulates SP-C's *in vitro* surface activity while overcoming many of the challenges related to natural SP-C. Peptoid-based analogues hold great potential for use in a synthetic, biomimetic LS formulation for treating RDS.

Graphical Abstract

*To whom correspondence should be addressed. Address: Stanford University, Department of Bioengineering, 443 Via Ortega, Shriram Center, Room 229, Stanford, CA 94305. Telephone: (650) 946-8039. aebarron@stanford.edu.

COMPETING INTERESTS

The authors declare no competing interests.

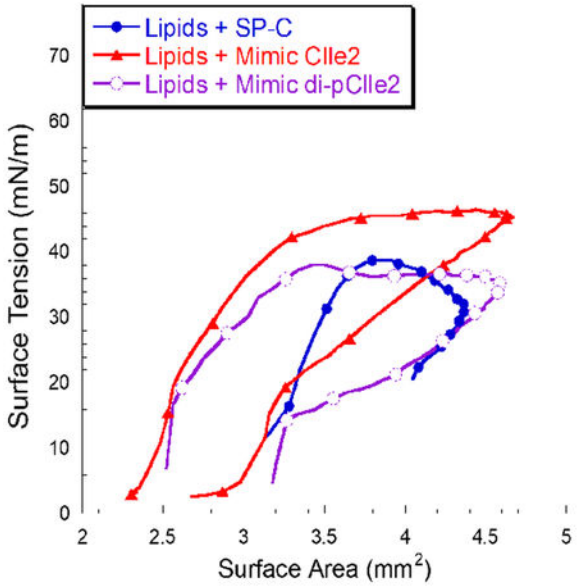

INTRODUCTION

Premature babies, that is those born with less than 28–32 weeks gestation, have a high incidence of respiratory distress as a result of underdeveloped lungs and a subsequent deficiency of functional lung surfactant (LS) material,[1–2] the thin mono-/multi-layer coating of lipids and proteins that lines the alveolar surfaces of vertebrate lungs. Infant respiratory distress syndrome (IRDS), once a primary cause of infant mortality in the United States, is now regularly treated with the instillation of exogenous surfactant material into the immature airways.[3] The exogenous surfactant functions in place of the native LS to maintain alveolar patency and to lessen the work of breathing until the patient is able to secrete functional LS. Despite the efficacy of these natural, animal-derived surfactant preparations, the potential for cross-species transfer of infectious agents, high production costs, and batch-to-batch variability continue to be ongoing concerns.[4] Surfactant replacement may benefit the treatment of other respiratory-related disorders for both infants and adults; however, to increase the applicability of surfactant replacement, a much greater quantity is needed at a reasonable cost.[5–6] These concerns and limited production potential have prompted the research and development of a synthetic surfactant formulation that can function like native LS.[7] However, this endeavor has been more daunting than originally anticipated, largely due to the difficulty in producing or mimicking the hydrophobic proteins of LS, surfactant proteins B and C (SP-B and SP-C).

While SP-B and SP-C represent only a small portion of LS (1–2 wt%), SP-B is critical for biophysical function[8] and SP-C is important for normal postnatal lung function.[9] LS, a complex biomaterial composed of approximately 10% proteins and 90% lipids, is essential for normal respiration. In the airways, this dynamic film functions to: 1) form an interfacial surfactant layer by rapidly adsorbing to the alveolar air-liquid interface, 2) prevent alveolar collapse by greatly reducing the interfacial surface tension upon compression to near-zero values (expiration), and 3) reduce the maximum surface tension and diminish the work of

breathing by efficiently respreading upon expansion (inhalation).[10] Dipalmitoyl phosphatidylcholine (DPPC), the primary lipid component of LS, along with the other saturated phospholipids, are the main surface tension-reducing entities in LS. The same biophysical properties that allow saturated phospholipids to achieve very low surface tensions also prevents them from rapidly reabsorbing and respreading upon expansion.[11] Adding fluid, unsaturated, or neutral phospholipids to LS improves respreading and slightly enhances LS adsorption to the air-liquid interface, but consequently increases minimum surface tension.[11–12] The addition of the hydrophobic proteins, SP-B and SP-C, to the lipid portion greatly enhances surfactant adsorption, stability, and recycling of the lipid film.[13–14] The inclusion of these surfactant-specific proteins is, therefore, necessary for proper respiration, as their omission results in lethal respiratory failure.[15–18]

SP-C is a helical and extraordinarily hydrophobic, 35-amino acid long protein that is highly sequenced-conserved amongst all mammalian species.[2, 19] Its 37-A° -long helical region is capable of traversing the lipid bilayer and associates and interacts with the interior of phospholipid acyl chains.[7] Additionally, the N-terminal region of natural SP-C contains two palmitoylated cysteines at positions 5 and 6 that are thought to play a key role in maintaining the association between SP-C and associated phospholipids with the interfacial surfactant film at very high levels of compression, acting as a hydrophobic “anchor” for the excluded surfactant material and aiding in the reincorporation of this material during expansion.[7, 20] Palmitoylation has also been shown to be vital in maintaining the rigid α-helical structure of SP-C.[21] The important biophysical activities of SP-C and its inclusion in animal-derived surfactants suggests that the protein is a critical constituent of a synthetic surfactant preparation; however, large-scale production is exceedingly difficult due to its highly hydrophobic nature.[4] While SP-C is relatively small and lacks any tertiary structure, the native protein and sequence-identical analogues are difficult to handle at all stages of experimentation. The poly-valyl helix is composed entirely of aliphatic residues with β-branched side chains that spontaneously convert into β-sheet aggregate structures with reduced surface activity in the absence of phospholipids.[22–24] The difficulties associated with native SP-C have led researchers to employ a number of different strategies to overcome its metastable secondary structure and aggregation propensity by producing SP-C mimics in heterologous systems, creating synthetic peptide analogues, and synthesizing non-natural peptidomimetics.[3–4, 25–28]

In designing an appropriate peptidomimetic, it is important to first consider what characteristics are essential to create a functional and more manageable SP-C analogue. SP-C structure-function studies have revealed certain necessary molecular features that retain SP-C’s functionality. SP-C’s extreme hydrophobicity, the longitudinally amphipathic patterning of hydrophobic and polar residues, and, most importantly, the maintenance of SP-C’s rigid, helical secondary structure are all crucial characteristics.[29–34] Many of SP-C’s surface-active properties are facilitated by the valyl-rich helical region, which approximates the thickness of a DPPC bilayer.[35] Several studies of synthetic mimics have focused on this region and found that the α-helical conformation, rather than the exact side chain chemistry, is of importance for capturing SP-C’s surface-active properties.[29–30, 32, 36–37] Therefore, it can be hypothesized that the requisite SP-C molecular parameters can be preserved with alternative yet equivalent side chain structures, thereby simplifying the production and

handling of SP-C analogues. Table 1 summarizes the key aspects of surface activity that can be evaluated *in vitro* for SP-C analogues by using complementary experimental techniques.

One approach to mimicking SP-C is the utilization of poly-*N*-substituted glycines or "peptoids".[30, 38–39] Peptoids are structurally similar to peptides, but the side chains are instead attached to the amide nitrogens rather than to the α-carbons. Peptoids are resistant to protease degradation and are more biostable than peptides as a result of this modified backbone.[40] They are also simple and cost-effective to synthesize relative to peptides.[41] The peptoid backbone is achiral and lacks backbone hydrogen bond donors; however, peptoids with α-chiral, sterically bulky side chains are capable of assuming extraordinarily stable, handed helices.[42–44] Peptoids are excellent candidates for mimicking bioactive molecules that rely on helical structure to properly function, such as the hydrophobic proteins of LS, because peptoids are able to form such stable helices.[39, 47–49] These helical structures are similar to a polyproline type I helix and have ~ 3 residues per turn with a helical pitch of ~ 6 Å.[45–46] Notably, many of the same design strategies used in the development of SP-C peptide-based analogues are also applicable to peptoid-based analogues.[39, 50] Similar to the peptide-based analogues, peptoid-based analogues containing a more rigid, aromatic-based helix display superior SP-C-like behaviors in comparison to peptoid-based analogues containing a more biomimetic, aliphatic-based helix, which suggests that the overall secondary structure of SP-C is the more important feature to mimic relative to the exact side chain chemistry.[30, 32]

Despite the superior surface activity of the aromatic-based mimics, the aliphatic-based mimics displayed some desirable properties, such as a lower maximum surface tension during dynamic cycling, indicating favorable interactions between the branched aliphatic side chains and the lipid acyl chains. The preservation of these interactions may be functionally important considering that the SP-C poly-valyl helix is conserved amongst all species studied thus far, but it is still unclear as to whether or not this is simply an adaption to the extremely hydrophobic lipid environment, or instead one of functional necessity.

To investigate the helical side chain properties further, a group of peptoid-based mimics were created and characterized to optimize the molecular features of both the α-chiral, aromatic and the α-chiral, aliphatic side chains (Figure 1). Specifically, the designed mimics contain varying amounts of aromatic and aliphatic residues in the 14-residue helical region (i.e., all-aromatic, 10 aromatic/4 aliphatic, and 5 aromatic/9 aliphatic side chains), imparting two molecular characteristics to one mimic by obtaining structural rigidity from the aromatic side chains and side chain biomimicry (i.e., Val-like structure) from the aliphatic side chains. We find that increasing the aliphatic content in the helical region incrementally increases the *in vitro* surface activity of the peptoid mimics, causing a reduction in maximum surface tension during dynamic cycling. With the incorporation of approximately one-third aromatic side chains for structural rigidity and two-thirds aliphatic side chains for side chain biomimicry in the helical region, the extents of rigidity and biomimicry were balanced and optimized, resulting in a mimic that displays superior surface activity than mimics composed solely of either aromatic or aliphatic side chains. To further improve the surface activity of the most promising mimic, two alkyl chains were introduced in the *N*-terminal region, following previous work.[51] The amide-linked C-18 alkyl chains mimic the structure and

hydrophobicity of the palmitoyl chains of SP-C that are responsible for important surface-active properties.[20, 35] Alkylation further improved the peptoid mimic's surface activity, resulting in a surfactant film with comparable *in vitro* surface activities to a natural SP-C-containing formulation.

MATERIALS AND METHODS

Materials.

Peptoid synthesis reagents, primary amines, and palmitic acid (PA) were purchased from Sigma-Aldrich (Milwaukee, WI). Fmoc-protected proline and Rink amide resin were obtained from NovaBiochem (San Diego, CA). Organic solvents for sample synthesis, purification, and preparation (HPLC-grade or better) were purchased from Fisher Scientific (Pittsburgh, PA). Synthetic phospholipids DPPC and palmitoyloleoyl phosphatidylglycerol (POPG) were purchased from Avanti Polar Lipids (Alabaster, AL) and used as received. Texas-Red® 1,2-dihexadecanoyl-sn-glycero-3-phosphoethanolamine, triethylammonium salt (TR-DHPE) was obtained from Molecular Probes (Eugene, OR). The native SP-C was a gift from Prof. Jesus Perez-Gil and was extracted from porcine LS utilizing the methodology of Perez-Gil et al.[52]

Peptoid synthesis.

The SP-C mimics (Table 2) were synthesized on a 433A ABI Peptide Synthesizer (Foster City, CA) on solid support, using the two-step submonomer protocol as previously described.[53] The crude products were purified by RP-HPLC on a Waters (Milford, MA) system with a Vydac C4 column and a linear gradient of 40–90% solvent B in solvent A over 80 minutes (solvent A = 0.1% TFA in water and solvent B = 0.1% TFA in isopropanol). The final purity of the peptoids was determined by analytical RP-HPLC to be > 97%. The correct molar masses were confirmed by electrospray ionization mass spectrometry (ESI/MS).

Circular dichroism spectroscopy.

Circular dichroism (CD) measurements were conducted using a Jasco model 715 spectropolarimeter (Easton, MD) with ~ 60 μM peptoid in methanol. CD spectra were acquired using a quartz cylindrical cell (Hellma model 121-QS, Forest Hills, NY) with a path length of 0.02 cm, employing a scan rate of 100 nm/min. CD spectra represent the average of 40 successive spectral accumulations. Data are reported in per-residue molar ellipticity (deg cm^2/dmol), as calculated per mole of amide groups present and normalized by the molar concentration of peptoid.

Langmuir-Wilhelmy surface balance and fluorescent microscopy.

Surface pressure-area isotherms were obtained using a home-built Langmuir-Wilhelmy surface balance (LWSB) with two straight Teflon barriers as previously described.[49] For each experiment, the subphase was filled with ~300 mL buffered subphase (150 mM NaCl, 5 mM $CaCl_2$ and 10 mM HEPES at pH 6.90) and heated to 37°C. A Wilhelmy surface balance (Reigler & Kirstein, Berlin, Germany) was then calibrated and used to monitor the surface pressure as the area of the trough was either expanded or compressed. The surfactant

material in an organic solution was spread at the air-liquid interface using a syringe, and solvent was allowed to evaporate for 10 minutes. The barriers were then compressed at a rate of 30 mm/min. Experiments were repeated at least six times with highly repeatable results.

Fluorescence microscopic (FM) images were obtained by using a Nikon MM40 compact microscope stand with a 100W mercury lamp (Tokyo, Japan) in conjunction with the LWSB. Fluorescence was detected by a Dage-MTI three-chip color camera (Dage-MTI, Michigan City, IN) in conjunction with a generation II intensifier (Fryer, Huntley, IL). Samples were spiked with 0.5 mol% of a fluorescently labeled lipid, TR-DHPE, for detection. Inclusion of the headgroup-labeled lipid at this concentration did not alter surfactant film morphology as previously shown.[54] FM experiments were also performed on aqueous buffered subphase at 37°C with a barrier speed of 5 mm/min. Lipid domain coverage and sizes were calculated using the ImageJ software (location) application.[55]

Pulsating bubble surfactometer.

Static and dynamic characterization of surfactant film properties were conducted on a modified PBS (General Transco, Largo, FL) as previously described,[56] using an imaging system to accurately track bubble size and shape throughout the experiment. The lipid mixture (DPPC:POPG:PA, 68:22:9 (by weight)) was dissolved in chloroform:methanol (3:1) alone or with 1.6 mol% SP-C additive, equivalent to 10 wt% total protein (or protein mimic) content (*i.e.*, total protein content of the final surfactant formulation), an SP-C concentration and lipid formulation successfully identified as optimal, and tested in previous *in vitro* and *in vivo* studies.[25, 38] The PBS samples were then dried under vacuum and re-suspended in an aqueous buffer solution (150 mM NaCl, 5 mM $CaCl_2$ and 10 mM HEPES at pH 6.90) to a lipid concentration of 1.0 mg/mL. Samples were then loaded into the PBS sample chamber using a modified leak-free methodology and placed on the PBS instrument at 37°C.[57] A bubble with a radius of 0.4 mm was then formed and an imaging acquisition system was used to determine the bubble size. For static adsorption experiments, trans-film bubble pressure was recorded as a function of time while holding the bubble radius static for 20 minutes. Dynamic measurements of surface tension as a function of bubble surface area were subsequently collected by cycling the bubble radius between approximately 0.4 mm and 0.55 mm at an oscillation frequency of 20 cycles/min (the adult respiratory rate) for 10 minutes. PBS experiments were repeated a minimum of six times for each preparation.

Statistical analysis.

One-way analysis of variance with post hoc Tukey-Kramer multiple comparison testing was used to analyze the results ($p < 0.05$).

RESULTS AND DISCUSSION

Peptoid design and rationale.

SP-C's biophysical activity is dominated by the presence of an extremely hydrophobic, rigid helix that contains only β-branch amino acids, predominately valine, leucine, and isoleucine. However, the replacement of SP-C's helix with the α-helical, transmembrane segment of bacteriorhodopsin does not alter SP-C's surface activity, indicating that the exact side chain

chemistry of this region is less important than the overall secondary structure of this region.[32, 58] An analogous finding was observed in peptoid-based analogues of SP-C, in which a rigid, aromatic helix better replicated the surface activity of a synthetic SP-C peptide than a more biomimetic, less structurally rigid aliphatic helix.[30] Despite the superiority of the aromatic-based helix, the aliphatic-based mimic displayed some favorable surface-active properties, including a lower maximum surface tension during dynamic cycling. This suggests a favorable interaction between the lipid acyl chains and the aliphatic side chains of the peptoid mimic.

To combine features of both side chain chemistries in one mimic, varying amounts of α-chiral, aliphatic (*N*ssb) and α-chiral, aromatic (*N*spe) monomers were incorporated into the helical region of a peptoid-based SP-C mimic. This strategy attempted to maintain stable helicity with the presence of the aromatic *N*spe side chains, while enhancing the degree of close biomimicry with the incorporation of the isoleucine-like side chains of the aliphatic *N*ssb residues. As both side chains are α-chiral, overall helical peptoid secondary structure is the predominant conformation of the backbone; yet with these differences in sequence come differences in structural dynamics. Previous fundamental studies of oligopeptoid secondary structure by CD and 2D-NMR[45–46, 59] have shown that *N*spe-rich peptoid helices are stabilized by interactions between the aromatic rings in the side chains with backbone carbonyls, while *N*ssb-rich helices, which lack those interactions, are more dynamic, alternating more frequently between *cis*-amide and *trans*-amide-dominated backbone conformers according to 2D-NMR, while still being overall helical as seen by CD.[45–46, 59] To state this more simply, *N*spe-rich peptoids are more strongly helical in structure (form a more rigid helix), while *N*ssb-rich peptoids will have a more biomimetic chemical structure, but more flexible helical structures.

The designed peptoid SP-C mimics are depicted in Table 2. Each of the analogues was designed to retain the longitudinally amphipathic patterning of polar and non-polar residues in SP-C as well as its helical secondary structure. The SP-C mimics comprised an achiral *N*-terminal region with side chain structures analogous to those of human SP-C, and a hydrophobic, α-chiral helical region, emulating the helical secondary structure of native SP-C. The helical region in these analogues contained either entirely aromatic residues (Mimic C), one-third aliphatic, isoleucine-like residues (Mimic CIle1), or two-thirds aliphatic residues (Mimic CIle2), creating a range from the most rigid (Mimic C) to the most biomimetic (Mimic CIle2). Because of the 3-residue periodicity of peptoid helices, the α-chiral, aliphatic and aromatic residues were positioned to align facially in the helical region so that Mimic CIle1 contained one aliphatic face and Mimic CIle2 contained two aliphatic faces. An entirely aliphatic mimic was not investigated, as previous studies have shown that this mimic was inferior overall in comparison to the aromatic-based mimic.[30] Two *N*-terminal alkyl chains were also incorporated into Mimic CIle2, resulting in Mimic di-pCIle2. These amide-linked C-18 alkyl chains mimic the length and hydrophobicity of the palmitoyl chains of SP-C, and have been found to positively impact the surface activity of a purely aromatic peptoid-based SP-C analogue.[51]

Circular dichroism.

SP-C's highly helical secondary structure in solution is a critical feature to capture in a synthetic mimic, as differences in helical content greatly affect SP-C's biophysical surface activity.[32] The secondary structure must also be stable over time in solution, which would significantly lessen the difficulty associated with handling the metastable protein. CD was conducted in methanol at ~60 μM and room temperature to characterize the secondary structure of the peptoid mimics (Figure 2). All the peptoid-based mimics exhibited spectral features consistent with helical structure. The spectrum for Mimic C was qualitatively similar to that of a peptide α-helix, with an intense maximum at ~ 192 nm and a double minimum at ~ 205 nm and ~ 220 nm, indicating a polyproline type-I-like peptoid helix and similar to other peptoids with chiral, aromatic side chains.[42, 44–45, 59] Increasing the aliphatic content in the helical region resulted in a CD spectrum that was progressively similar to a typical polyproline type I peptide helix. The CD spectra for Mimics CIle1, CIle2, and di-pCIle2 contained a minimum at ~ 220 nm that became progressively weaker in this order, and the local minimum at ~ 205 nm was gradually shifted towards shorter wavelengths. A local maximum was also observed at ~ 208 nm. The degree of spectral shift coincided with the amount of helix-inducing aliphatic side chains present within Mimic CIle2 and Mimic di-pCIle2, and these mimics displayed spectra that were most similar to a polyproline type I helix. The presence of the alkyl chains in the peptoid analogue di-pCIle2 decreased the minimum at ~ 220 nm, but otherwise, the CD spectrum was very similar to that of the unalkylated mimic (Mimic CIle2) and did not notably affect the secondary structure of the peptoid mimic. Overall, the peptoid mimics were all structured and helical in solution.

Langmuir-Wilhelmy surface balance.

To determine the influence of the peptoid analogues on the monolayer phase behavior of a lipid film, SP-C mimics were added at 1.6 mol% to an optimized lipid formulation consisting of DPPC:POPG:PA (68:22:9, by weight). This formulation closely mimics the behaviors of the lipid portion of LS.[38, 60] The resulting surfactant formulations were analyzed on the LWSB as previously described.[49] The surface pressure-area LWSB isotherms at 37°C for the lipids alone, lipids with natural SP-C, and lipids with the peptoid analogues are shown in Figure 3.

In typical LWSB isotherms of LS, the material is initially spread at the air-liquid interface in the gaseous phase, where there are few interactions between molecular species and no change in surface pressure. As the trough area available to the molecules is decreased with compression of the barriers, the molecules are in closer proximity, and start interacting with each other, forming a uniform liquid expanded (LE) phase. The initial increase in surface pressure (decrease in surface tension) observed at this point is termed "lift-off." An early lift-off (> 100 $Å^2$/molecule) is an important characteristic of LS.[61] Further compression of the interfacial surfactant layer causes increased interactions amongst the surfactant species and an increase in surface pressure leading to the coexistence of the LE and liquid condensed (LC) phases. As the surface layer is compressed further, a biomimetic plateau region in the isotherm is observed between 40–55 mN/m. This is likely due to the reversible removal and rearrangement of the material from the interface, forming a metastable

surfactant layer, which is more pronounced in the presence of SP-C.[62–63] Eventually, the surface layer reaches a state of compression where the interfacial layer can no longer accommodate a further reduction in surface area without being excluded from the interface. LS has a very high maximum surface pressure near 72 mN/m, corresponding to a low surface tension of ~ 0 mN/m.

Figure 3A shows that the LWSB isotherm for the lipid only formulation has a lift-off point of ~ 85 $Å^2$/molecule. The slope of the isotherm was relatively small up to a surface pressure of ~12 mN/m, indicating high compressibility that is typical of the LE phase. The slope of the isotherm increased as the surface layer was further compressed from 12 mN/m to ~ 48 mN/m, indicating a less compressible film.[64–65] A slight shift in the isotherm at ~ 50 mN/m and a collapse pressure of ~ 72 mN/m was observed upon further compression of the lipid film. Introducing porcine SP-C to the lipid formulation dramatically altered the surface pressure-area isotherm characteristics. The lift-off shifted to a greater molecular area (~ 97 $Å^2$/molecule vs. ~ 85 $Å^2$/molecule), which indicates increased surface activity due to the existence of SP-C in the interfacial surfactant layer. At lower surface pressures, the isotherm was similar to the lipids alone, but shifted towards a larger molecular area. A pronounced biomimetic plateau region beginning at ~ 42 mN/m was seen after further compression. This is likely due to the reversible removal of lipid and protein from the surface layer, creating a surface-associated, surfactant reservoir.[62] This surfactant reservoir may explain how SP-C can interact with lipids, allowing for low surface tension upon compression and respreading rapidly on expansion.[66–67] After additional compression of the SP-C containing formulation, a similar collapse pressure of ~ 72 mN/m was observed.

Adding Mimic C to the lipid formulation resulted in a LWSB isotherm that is nearly identical to the SP-C formulation, with a similar lift-off point of ~ 96 $Å^2$/molecule and a pronounced plateau at ~ 43 mN/m (Figure 3A). Adding one aliphatic face to the helical region, Mimic CIle1, similarly altered the surfactant film characteristics of the lipid formulation, but with some variation in the plateau region (Figure 3B). Lift-off is also shifted to greater molecular area, ~ 95 $Å^2$/molecule, than compared to lipids alone; however, the plateau region is different than that observed for formulations containing either SP-C or Mimic C. The Mimic CIle1 formulation displayed an altered plateau region from surface pressures ~ 43 mN/m to ~ 50 mN/m, the extent of which is as equally pronounced as the plateau region for formulations SP-C and Mimic C. Adding Mimic CIle2 and Mimic di-pCIle2 also resulted in a similar isotherm with a lift-off of ~ 95 $Å^2$/molecule for both formulations. The plateau region of these isotherms is more similar to the SP-C and Mimic C-containing films, with only one kink in the isotherm occurring at ~ 43 mN/m for Mimic CIle2, and ~ 47 mN/m for Mimic di-pCIle2. The increase in the plateau pressure for the alkylated mimic is consistent with studies of an alkylated, aromatic peptoid mimic of SP-C.[51] The formulations containing Mimic CIle2 and di-pCIle2 also had a high collapse pressure of ~ 72 mN/m.

Fluorescent microscopy.

To further investigate the influence of SP-C and the peptoid-based SP-C mimics on the monolayer phase behavior, FM was used to characterize the surface film morphology as a

function of surface pressure for the surfactant formulations. FM provides direct visualization of the surfactant monolayer at the air-liquid interface, enabling analysis of the impact the added species have on the creation and transition of the surfactant domain structures. Figure 4 displays the FM images obtained at 37°C at ~ 35 mN/m and ~ 50 mN/m for lipids alone, with SP-C, and with the peptoid mimics.

Below the plateau region in the LWSB isotherm at a surface pressure of ~ 35 mN/m, all surfactant formulations exhibited film morphologies that were similar, with the coexistence of a bright, fluid LE phase with dark LC phases. The film coverage and LC domain size (53–65 μm^2) were similar for all the formulations except the SP-C-containing formulation, which had much smaller LC domains, ~ 25 μm^2. Above the plateau region at ~ 50 mN/m, the film morphologies and trends in LC size were similar to those seen at ~ 35 mN/m except that bright, vesicle-like protrusions were now present for all of the surfactant formulations excluding the lipids alone. These protrusions likely corresponded to removal of surfactant material from the interface and the formation of a surface-associated surfactant reservoir. Their formation in the SP-C and SP-C mimic-containing films is also supported by the pronounced plateau region in the LWSB isotherms. All the peptoid-containing films displayed similar morphology to the SP-C film although the native protein was better able to condense the size of the LC domains.

Static-bubble adsorption.

Native LS initially dispersed in an aqueous subphase rapidly adsorbs to the air-liquid interface, reaching a surface tension below 25 mN/m in less than a minute.[56, 68] This rapid adsorption is an essential biophysical characteristic to mimic with a synthetic LS formulation, and is improved by the inclusion of SP-C and SP-B.[2, 10] The static-bubble adsorption kinetics of the lipid mixture alone, lipids with 1.6 mol% SP-C, and lipids with 1.6 mol% SP-C peptoid analogues, were characterized with a modified PBS run in static-bubble mode with a bubble radius of approximately 0.40 mm at 37°C. Figure 5 shows the adsorption surface tension as a function of time for the different surfactant formulations.

Without any of the SP-C-like species, the lipid mixture displayed very slow surface adsorption and failed to achieve an equilibrium surface tension lower than ~ 50 mN/m even after 20 minutes of static adsorption. Adding SP-C to the lipid formulation dramatically improved the static adsorption kinetics, reaching an adsorption surface tension below 30 mN/m in less than a minute and a final surface tension of ~ 26 mN/m. All of the peptoid mimics similarly improved the surface adsorption of the lipid formulation. The formulations containing Mimics C, CIle1, CIle2, and di-pCIle2 all reached a static surface tension below 30 mN/m in less than one minute and a final surface tension of ~ 24–27 mN/m. The peptoid mimics appeared to enable adsorption and insertion of the dispersed surfactant material to the air-liquid interface in a manner very similar to SP-C. The presence of the aliphatic side chains in the helical region did not significantly alter the adsorption profile, which was somewhat surprising given that an entirely aliphatic peptoid mimic previously did not display favorable adsorption in a synthetic lipid formulation.[30] It is hypothesized that the presence of the aromatic side chains in the helical region increased the rigidity of this region

due to increased steric and electronic repulsions between adjacent side chains, facilitating disruption and fusion of the dispersed surfactant structures to the air-liquid interface.

Dynamic-bubble cycling.

Once at the air-liquid interface, LS exhibits several features that are important to mimic during dynamic compression and expansion cycles. These features include: (1) achieving a very low surface tension with a small amount of compression; (2) respreading rapidly upon expansion, and (3) controlling surface tension as a function of bubble surface area with a very low minimum surface tension (near–zero mN/m) and a low maximum surface tension.[2, 10] In order to investigate the ability of the peptoid-based SP-C formulations to reduce and control surface tension as a function of surface area, PBS experiments were conducted at 37°C in a dynamic mode with an oscillation frequency of 20 cycles/min (the approximate adult respiratory rate) and ~ 50% reduction in surface area per cycle. Figure 6 shows surface tension as a function of bubble surface area for lipid mixtures with and without SP-C and the peptoid analogues.

The lipid formulation without any added SP-C species was unable to reduce the surface tension below ~ 13 mN/m during compression and, upon expansion, the maximum surface tension rose to ~ 61 mN/m. Also, a large amount of compression was required for the lipid formulation to reach its lowest surface tension. These dynamic compression-expansion characteristics are not acceptable for a biomimetic LS formulation. The addition of SP-C to the lipid formulation resulted in surface-active features that were significantly improved relative to the lipid formulation alone. Both the minimum and maximum surface tensions were significantly lower, < 1 mN/m and ~ 39 mN/m, respectively. The surfactant film with SP-C was also much less compressible, requiring less compression to reach a low surface tension.

The addition of the peptoid-based SP-C mimics to the lipid formulation also resulted in an improvement of the lipid formulation's surface-active features during dynamic cycling with all formulations reaching near-zero surface tension. The presence of Mimic C caused a reduction in the maximum and minimum surface tensions to ~ 53 mN/m and <1 mN/m, respectively. These improvements were significant over the lipid formulation, but the maximum surface tensions were inferior relative to the formulation containing native SP-C. Adding one aliphatic face into the helical region (Mimic CIle1) resulted in a compression-expansion loop that was very similar to Mimic C, but with the maximum surface tension slightly reduced to ~ 50 mN/m. The introduction of a second α-chiral, aliphatic face into the helical region (Mimic CIle2) further improved the dynamic compression-expansion film behavior, resulting in a maximum surface tension of ~ 47 mN/m. The reduction in maximum surface tension indicated that the inclusion of aliphatic side chains in the helical region promoted favorable interactions between the hydrophobic helices of the peptoid analogues and the lipid acyl chains. This interaction may increase the aliphatic-containing peptoid mimics' association with excluded surfactant material through increased lipid affinity, better enabling the reincorporation of this material upon expansion and reducing the maximum surface tension. The presence of the α-chiral, aromatic side chains was previously found to be necessary for activity in peptoid-based mimics, as their removal led to a surfactant film

that required a significant amount of compression to reach a low surface tension.[30] By creating a mimic, Mimic CIle2, that utilizes features of both aromatic and aliphatic side chain chemistries, the structural and biomimetic requirements of the hydrophobic helical region were balanced, and the surface activity of the SP-C mimic was thus optimized. It is possible that an all-aromatic mimic may be easily excluded from insertion into the lipid bilayer, whereas some aromatic character may allow a mimic to keep its rigidity but stay inserted due to the aliphatic chains.

Despite the much-improved surface activity, Mimic CIle2 did not fully replicate the very low maximum surface tension exhibited by the SP-C-containing surfactant film (Figure 6). This is likely due to the presence of the two palmitoyl chains in positions 5 and 6 in the *N*-terminal region of natural SP-C that promote interactions with the phospholipids. When two alkyl chains were added to the *N*-terminal region of Mimic CIle2 (Mimic di-pCIle2) to mimic this palmitoylation, it was found that the maximum surface tension during dynamic cycling was dramatically reduced to ~ 39 mN/m (Figure 6B). Lift-off area did not change though (Figure 3B), demonstrating that the alkylated chains were well-incorporated into the film. Both the maximum and minimum surface tensions of the Mimic di-pCIle2 formulation were comparable to the SP-C formulation, with no statistically significant difference between maximum surface tension values, making Mimic di-pCIle2 a promising candidate for use in a biomimetic LS formulation.

CONCLUSIONS

The *C*-terminal hydrophobic helix of SP-C has been shown to greatly influence SP-C's many reported interactions and surface activities in a phospholipid environment; however, because of the high content of β-branched amino acids, the helix is metastable in solution and prone to misfolding and aggregating into inactive, non-helical conformations.[24, 58] One strategy to address this challenge is by mimicking SP-C with poly-*N*-substituted glycines or "peptoids".[30, 38–39] Peptoids with α-chiral, sterically bulky side chains are able to adopt stable, handed helices,[42–44] making them excellent candidates for biomimicry of the hydrophobic proteins of LS.[39, 47–49] In prior work, peptoid mimics utilizing structurally rigid, aromatic residues in the helical region were found to have superior SP-C-like behaviors than more biomimetic analogues containing a less structurally rigid, aliphatic helix.[30] However, the aliphatic-based peptoid mimics did display a lower maximum surface tension during dynamic cycling. This suggests a potential interaction between the lipid acyl chains and the aliphatic side chains of the peptoid helix. To investigate this possibility, a set of peptoid-based SP-C analogues was created, incorporating both aromatic and aliphatic residues in the helical region to combine the structural features of the aromatic residues and biomimetic features of the aliphatic residues in one SP-C mimic, while still retaining the helical secondary structure.

CD spectroscopy studies of the synthetic analogues showed that all the peptoid-based mimics were structured (helical) in solution. The surface activities of these analogues in a surfactant lipid film were characterized *in vitro* using LWSB, FM, and PBS, and compared to native porcine SP-C. All the peptoid analogues displayed favorable surface-active features when combined with a synthetic lipid formulation, and overall, the results from LWSB, FM,

and static PBS experiments were similar among the mimics. However, increasing the aliphatic content of the helical region increased the surface activity of the peptoid mimics by incrementally decreasing the maximum surface tension. The surfactant containing Mimic CIle2 displayed the lowest maximum surface tension during dynamic cycling while retaining a low compressibility due to the aromatic side chains. These studies revealed that both the side chain chemistry and the rigid secondary structure of the helical region were important components of an analogue of SP-C that contains Ile-like side chains. A structurally rigid helix resulted in a less compressible film, requiring less compression to reach a minimum surface tension while side chain biomimicry dramatically reduced the maximum surface tension of a dynamically cycled film in a stepwise fashion. To further improve the biomimicry and activity of Mimic CIle2, two alkyl chains were included in the *N*-terminal region. These amide-linked alkyl chains were similar to the palmitoyl chains of natural SP-C. This modification dramatically reduced the maximum surface tension of the surfactant formulation and was comparable to natural SP-C, the first time this milestone has been achieved by a peptoid mimic. Therefore, the structural and biomimetic features of SP-C in this peptoid analogue was enhanced by combining the optimal molecular and structural characteristics of both the helical *C*-terminal region and the amphipathic *N*-terminal region into one design.

Additional characterization experiments would investigate peptoid orientation in membranes using X-ray reflectivity (XR) studies.[69] Other recent work has revealed that the activity of both SP-B and SP-C surfactant proteins is related with the formation of supramolecular protein complexes, and in future work using both types of mimics, this could be investigated.[70] Techniques such as analytical ultracentrifugation (AUC) can be used to evaluate peptoid oligomerization. The presence of aromatic sidechains would likely facilitate the formation of self-associated peptoid oligomers.

The metabolic fate of these peptoid mimics when delivered to the lung is not yet established. A clearer understanding of peptoid mechanism of clearance will be important as these mimics are further developed for *in vivo* applications in the lung. Prior work on helical, amphipathic, antimicrobial peptoids used *in vivo* to treat an intraperitoneal infection, did show that these peptoids were well-tolerated (*i.e.*, no apparent acute negative effects, and no apparent immune response).[71] When delivered systemically per oral, intravenously, or intraperitoneally,[64]Cu-labeled antimicrobial peptoids in general exhibited higher *in vivo* stability and tissue accumulation and slower elimination in comparison to peptides.[72] A recent study compared the metabolic fate of poractant alfa to a synthetic, peptide-based surfactant, CHF5633, by tracking the fate of carbon 13-labelled DPPC.[73] While we expect that our peptoid mimics will be more resistant to protease degradation compared to peptides, further studies would be needed to determine the metabolic fate of a peptoid-based surfactant therapy (i.e., peptoid mimics + lipids). Recently, a mono-alkylated (single *N*ocd residue) variant of Mimic C was tested in an *in vivo* rat model of acute lung injury.[25] The peptoid-based surfactants were comparable to an animal derived surfactant (BLES) in terms of physiological and biochemical outcomes. In fact, the SP-C mimic alone formulation appeared to perform slightly better than BLES in terms of blood oxygen level and Alveolar-arterial (A-a) gradient. Future *in vivo* studies would test other promising SP-C mimic designs (e.g., Mimic di-pCIle2) for efficacy. Overall, peptoid-based analogues hold great

potential for use in a synthetic, biomimetic LS formulation for treating respiratory distress-related disorders.

ACKNOWLEDGMENTS

We thank Prof. Jesus Perez-Gil for the gift of porcine SP-C as well as Dr. Mark Johnson and Dr. Ronald Zuckermann for their assistance. Also, NJB is grateful to Dr. Michelle Dohm and Dr. Shannon Seurynck-Servoss for their assistance and insight. NJB acknowledges support from the NIH Biotechnology Training Program and US National Institutes of Health (Grant 2 R01 HL067984). We also acknowledge use of the Keck Biophysics facility at Northwestern University for CD measurements. The Molecular Foundry has also provided support for this project; work at the Molecular Foundry was supported by the Office of Science, Office of Basic Energy Sciences, of the U.S. Department of Energy under Contract No. DE-AC02–05CH11231.

Glossary

LS	lung surfactant
SP-C	surfactant protein C
IRDS	infant respiratory distress syndrome
LWSB	Langmuir-Wilhelmy Surface Balance
FM	fluorescence microscop
PBS	Pulsating Bubble Surfactometer
LE	liquid expanded
LC	liquid condensed

REFERENCES

1. Avery ME; Mead J, Surface properties in relation to atelectasis and hyaline membrane disease. AMA J Dis Child 1959, 97 (5, Part 1), 517–23. [PubMed: 13649082]
2. Notter RH, Lung Surfactants: Basic Science and Clinical Applications Marcel Dekker, Inc: New York, 2000; Vol. 149.
3. Mingarro I; Lukovic D; Vilar M; Perez-Gil J, Synthetic pulmonary surfactant preparations: new developments and future trends. Curr Med Chem 2008, 15 (4), 393–403. [PubMed: 18288994]
4. Curstedt T; Johansson J, New synthetic surfactant - How and when? Biology of the Neonate 2006, 89 (4), 336–339. [PubMed: 16770074]
5. Spragg R, Surfactant for acute lung injury. American journal of respiratory cell and molecular biology 2007, 37 (4), 377–8. [PubMed: 17872593]
6. Spragg RG; Lewis JF; Walmrath H; Johannigman J; Bellingan G; Laterre P; Witte MC; Richards GA; Rippin G; Rathgeb F; Hafner D; Taut FJH; Seeger W, Effect of recombinant surfactant protein C-based surfactant on the acute respiratory distress syndrome. New England Journal of Medicine 2004, 351 (9), 884–892. [PubMed: 15329426]
7. Brown NJ; Johansson J; Barron AE, Biomimicry of surfactant protein C. Accounts of chemical research 2008, 41 (10), 1409–17. [PubMed: 18834153]
8. Weaver TE; Conkright JJ, Functions of surfactant proteins B and C. Annual Review of Physiology 2001, 63, 555–578.
9. Nogee LM; Dunbar AE 3rd; Wert SE; Askin F; Hamvas A; Whitsett JA, A mutation in the surfactant protein C gene associated with familial interstitial lung disease. N Engl J Med 2001, 344 (8), 573–9. [PubMed: 11207353]

10. Johansson J; Curstedt T; Robertson B, Artificial surfactants based on analogues of SP-B and SP-C. Pediatr Pathol Mol Med 2001, 20 (6), 501–18. [PubMed: 11699576]
11. Veldhuizen R; Nag K; Orgeig S; Possmayer F, The role of lipids in pulmonary surfactant. Biochim Biophys Acta 1998, 1408 (2–3), 90–108. [PubMed: 9813256]
12. Gomez-Gil L; Schurch D; Goormaghtigh E; Perez-Gil J, Pulmonary surfactant protein SP-C counteracts the deleterious effects of cholesterol on the activity of surfactant films under physiologically relevant compression-expansion dynamics. Biophys J 2009, 97 (10), 2736–45. [PubMed: 19917227]
13. Hall SB; Venkitaraman AR; Whitsett JA; Holm BA; Notter RH, Importance of Hydrophobic Apoproteins as Constituents of Clinical Exogenous Surfactants. American Review of Respiratory Disease 1992, 145 (1), 24–30. [PubMed: 1731593]
14. Wang Z; Hall SB; Notter RH, Roles of different hydrophobic constituents in the adsorption of pulmonary surfactant. J Lipid Res 1996, 37 (4), 790–8. [PubMed: 8732779]
15. Clark JC; Wert SE; Bachurski CJ; Stahlman MT; Stripp BR; Weaver TE; Whitsett JA, Targeted disruption of the surfactant protein B gene disrupts surfactant homeostasis, causing respiratory failure in newborn mice. Proc Natl Acad Sci U S A 1995, 92 (17), 7794–8. [PubMed: 7644495]
16. Nogee LM; de Mello DE; Dehner LP; Colten HR, Brief report: deficiency of pulmonary surfactant protein B in congenital alveolar proteinosis. N Engl J Med 1993, 328 (6), 406–10. [PubMed: 8421459]
17. Nogee LM; Wert SE; Proffit SA; Hull WM; Whitsett JA, Allelic heterogeneity in hereditary surfactant protein B (SP-B) deficiency. Am J Respir Crit Care Med 2000, 161 (3 Pt 1), 973–81. [PubMed: 10712351]
18. Vorbroker DK; Profitt SA; Nogee LM; Whitsett JA, Aberrant processing of surfactant protein C in hereditary SP-B deficiency. Am J Physiol 1995, 268 (4 Pt 1), L647–56. [PubMed: 7537464]
19. Foot NJ; Orgeig S; Donnellan S; Bertozzi T; Daniels CB, Positive selection in the N-terminal extramembrane domain of lung surfactant protein C (SP-C) in marine mammals. J Mol Evol 2007, 65 (1), 12–22. [PubMed: 17568982]
20. Gonzalez-Horta A; Andreu D; Morrow MR; Perez-Gil J, Effects of palmitoylation on dynamics and phospholipid-bilayer-perturbing properties of the N-terminal segment of pulmonary surfactant protein SP-C as shown by 2H-NMR. Biophys J 2008, 95 (5), 2308–17. [PubMed: 18502795]
21. Wang ZD; Gurel O; Baatz JE; Notter RH, Acylation of pulmonary surfactant protein-C is required for its optimal surface active interactions with phospholipids. Journal of Biological Chemistry 1996, 271 (32), 19104–19109. [PubMed: 8702584]
22. Kallberg Y; Gustafsson M; Persson B; Thyberg J; Johansson J, Prediction of amyloid fibril-forming proteins. J Biol Chem 2001, 276 (16), 12945–50. [PubMed: 11134035]
23. Szyperski T; Vandenbussche G; Curstedt T; Ruysschaert JM; Wuthrich K; Johansson J, Pulmonary surfactant-associated polypeptide C in a mixed organic solvent transforms from a monomeric alpha-helical state into insoluble beta-sheet aggregates. Protein Science 1998, 7 (12), 2533–2540. [PubMed: 9865947]
24. Gustafsson M; Thyberg J; Naslund J; Eliasson E; Johansson J, Amyloid fibril formation by pulmonary surfactant protein C. FEBS Lett 1999, 464 (3), 138–42. [PubMed: 10618493]
25. Czyzewski AM; McCaig LM; Dohm MT; Broering LA; Yao LJ; Brown NJ; Didwania MK; Lin JS; Lewis JF; Veldhuizen R; Barron AE, Effective in vivo treatment of acute lung injury with helical, amphipathic peptoid mimics of pulmonary surfactant proteins. Scientific reports 2018, 8 (1), 6795. [PubMed: 29717157]
26. Notter RH; Gupta R; Schwan AL; Wang Z; Shkoor MG; Walther FJ, Synthetic lung surfactants containing SP-B and SP-C peptides plus novel phospholipase-resistant lipids or glycerophospholipids. PeerJ 2016, 4, e2635. [PubMed: 27812430]
27. Bae CW; Chung SH; Choi YS, Development of a Synthetic Surfactant Using a Surfactant Protein-C Peptide Analog: In Vitro Studies of Surface Physical Properties. Yonsei Med J 2016, 57 (1), 203–8. [PubMed: 26632402]
28. Seehase M; Collins JJ; Kuypers E; Jellema RK; Ophelders DR; Ospina OL; Perez-Gil J; Bianco F; Garzia R; Razzetti R; Kramer BW, New surfactant with SP-B and C analogs gives survival benefit after inactivation in preterm lambs. PLoS One 2012, 7 (10), e47631. [PubMed: 23091635]

29. Almlen A; Stichtenoth G; Robertson B; Johansson J; Curstedt T, Concentration dependence of a poly-leucine surfactant protein C analogue on in vitro and in vivo surfactant activity. Neonatology 2007, 92 (3), 194–200. [PubMed: 17476119]
30. Brown NJ; Wu CW; Seurynck-Servoss SL; Barron AE, Effects of hydrophobic helix length and side chain chemistry on biomimicry in peptoid analogues of SP-C. Biochemistry 2008, 47 (6), 1808–18. [PubMed: 18197709]
31. Creuwels L; Boer EH; Demel RA; Vangolde LMG; Haagsman HP, Neutralization of the Positive Charges of Surfactant Protein-C - Effects on Structure and Function. Journal of Biological Chemistry 1995, 270 (27), 16225–16229. [PubMed: 7608188]
32. Johansson J; Nilsson G; Stromberg R; Robertson B; Jornvall H; Curstedt T, Secondary Structure and Biophysical Activity of Synthetic Analogs of the Pulmonary Surfactant Polypeptide Sp-C. Biochem J 1995, 307, 535–541. [PubMed: 7733894]
33. Johansson J; Szyperski T; Wuthrich K, Pulmonary surfactant-associated polypeptide SP-C in lipid micelles: CD studies of intact SP-C and NMR secondary structure determination of depalmitoyl-SP-C(1–17). FEBS Lett 1995, 362 (3), 261–5. [PubMed: 7729509]
34. Takei T; Hashimoto Y; Aiba T; Sakai K; Fujiwara T, The surface properties of chemically synthesized peptides analogous to human pulmonary surfactant protein SP-C. Biol Pharm Bull 1996, 19 (10), 1247–53. [PubMed: 8913491]
35. Plasencia I; Keough KM; Perez-Gil J, Interaction of the N-terminal segment of pulmonary surfactant protein SP-C with interfacial phospholipid films. Biochim Biophys Acta 2005, 1713 (2), 118–28. [PubMed: 16002041]
36. Nilsson G; Gustafsson M; Vandenbussche G; Veldhuizen E; Griffiths WJ; Sjovall J; Haagsman HP; Ruysschaert JM; Robertson B; Curstedt T; Johansson J, Synthetic peptide-containing surfactants--evaluation of transmembrane versus amphipathic helices and surfactant protein C poly-valyl to poly-leucyl substitution. Eur J Biochem 1998, 255 (1), 116–24. [PubMed: 9692909]
37. Takei T; Hashimoto Y; Ohtsubo E; Sakai K; Ohkawa H, Characterization of poly-leucine substituted analogues of the human surfactant protein SP-C. Biol Pharm Bull 1996, 19 (12), 1550–5. [PubMed: 8996637]
38. Seurynck-Servoss Brown, N. J.; Dohm MT; Wu CW; Barron AE, Lipid composition greatly affects the in vitro surface activity of lung surfactant protein mimics. Colloids and Surfaces B-Biointerfaces 2007, 57 (1), 37–55.
39. Wu CW; Seurynck SL; Lee KY; Barron AE, Helical peptoid mimics of lung surfactant protein C. Chem Biol 2003, 10 (11), 1057–63. [PubMed: 14652073]
40. Miller SM; Simon RJ; Ng S; Zuckermann RN; Kerr JM; Moos WH, Comparison of the Proteolytic Susceptibilities of Homologous L-Amino-Acid, D-Amino-Acid, and N-Substituted Glycine Peptide and Peptoid Oligomers. Drug Development Research 1995, 35 (1), 20–32.
41. Czyzewski AM; Barron AE, Protein and peptide biomimicry: Gold-mining inspiration from Nature's ingenuity. Aiche J 2008, 54 (1), 2–8.
42. Kirshenbaum K; Barron AE; Goldsmith RA; Armand P; Bradley EK; Truong KT; Dill KA; Cohen FE; Zuckermann RN, Sequence-specific polypeptoids: a diverse family of heteropolymers with stable secondary structure. Proc Natl Acad Sci U S A 1998, 95 (8), 4303–8. [PubMed: 9539732]
43. Sanborn TJ; Wu CW; Zuckerman RN; Barron AE, Extreme stability of helices formed by water-soluble poly-N-substituted glycines (polypeptoids) with alpha-chiral side chains. Biopolymers 2002, 63 (1), 12–20. [PubMed: 11754344]
44. Wu CW; Sanborn TJ; Huang K; Zuckermann RN; Barron AE, Peptoid oligomers with alpha-chiral, aromatic side chains: sequence requirements for the formation of stable peptoid helices. J Am Chem Soc 2001, 123 (28), 6778–84. [PubMed: 11448181]
45. Armand P; Kirshenbaum K; Goldsmith RA; Farr-Jones S; Barron AE; Truong KT; Dill KA; Mierke DF; Cohen FE; Zuckermann RN; Bradley EK, NMR determination of the major solution conformation of a peptoid pentamer with chiral side chains. Proc Natl Acad Sci U S A 1998, 95 (8), 4309–14. [PubMed: 9539733]
46. Wu CW; Kirshenbaum K; Sanborn TJ; Patch JA; Huang K; Dill KA; Zuckermann RN; Barron AE, Structural and spectroscopic studies of peptoid oligomers with alpha-chiral aliphatic side chains. J Am Chem Soc 2003, 125 (44), 13525–30. [PubMed: 14583049]

47. Seurynck-Servoss SL; Dohm MT; Barron AE, Effects of including an N-terminal insertion region and arginine-mimetic side chains in helical peptoid analogues of lung surfactant protein B. Biochemistry 2006, 45 (39), 11809–18. [PubMed: 17002281]
48. Dohm MT; Seurynck-Servoss SL; Seo J; Zuckermann RN; Barron AE, Close mimicry of lung surfactant protein B by "clicked" dimers of helical, cationic peptoids. Biopolymers 2009, 92 (6), 538–53. [PubMed: 19777571]
49. Seurynck SL; Patch JA; Barron AE, Simple, helical peptoid analogs of lung surfactant protein B. Chem Biol 2005, 12 (1), 77–88. [PubMed: 15664517]
50. Brown NJ; Seurynck SL; Wu CW; Johnson M; Barron AE, Effect of the hydrophobic helix length on biomimiery in peptoid analogues of SP-C. Biophysical Journal 2005, 88 (1), 576a–577a.
51. Brown NJ; Dohm MT; Bernardino de la Serna, J.; Barron, A. E., Biomimetic N-terminal alkylation of peptoid analogues of surfactant protein C. Biophys J 2011, 101 (5), 1076–85. [PubMed: 21889444]
52. Perezgil J; Cruz A; Casals C, Solubility of Hydrophobic Surfactant Proteins in Organic-Solvent Water Mixtures - Structural Studies on Sp-B and Sp-C in Aqueous-Organic Solvents and Lipids. Biochimica Et Biophysica Acta 1993, 1168 (3), 261–270. [PubMed: 8323965]
53. Zuckermann RN; Kerr JM; Kent SBH; Moos WH, Efficient method for the preparation of peptoids [oligo(N-substituted glycines)] by submonomer solid-phase synthesis. J Am Chem Soc 1992, 114 (26), 10646–10647.
54. Bringezu F; Ding JQ; Brezesinski G; Zasadzinski JA, Changes in model lung surfactant monolayers induced by palmitic acid. Langmuir 2001, 17 (15), 4641–4648.
55. Abramoff MD; Magelhaes PJ; Ram SJ, Image Processing with ImageJ. Biophotonics Internation 2004, 11 (7), 36–42.
56. Seurynck SL; Brown NJ; Wu CW; Germino KW; Kohlmeir EK; Ingenito EP; Glucksberg MR; Barron AE; Johnson M, Optical monitoring of bubble size and shape in a pulsating bubble surfactometer. J Appl Physiol (1985) 2005, 99 (2), 624–33. [PubMed: 15790687]
57. Putz G; Goerke J; Taeusch HW; Clements JA, Comparison of Captive and Pulsating Bubble Surfactometers with Use of Lung Surfactants. Journal of Applied Physiology 1994, 76 (4), 1425–1431. [PubMed: 8045815]
58. Clercx A; Vandenbussche G; Curstedt T; Johansson J; Jornvall H; Ruysschaert JM, Structural and functional importance of the C-terminal part of the pulmonary surfactant polypeptide SP-C. Eur J Biochem 1995, 229 (2), 465–72. [PubMed: 7744069]
59. Wu CW; Sanborn TJ; Zuckermann RN; Barron AE, Peptoid oligomers with alpha-chiral, aromatic side chains: effects of chain length on secondary structure. J Am Chem Soc 2001, 123 (13), 2958–63. [PubMed: 11457005]
60. Tanaka Y; Takei T; Aiba T; Masuda K; Kiuchi A; Fujiwara T, Development of synthetic lung surfactants. J Lipid Res 1986, 27 (5), 475–85. [PubMed: 3755458]
61. Alonso C; Alig T; Yoon J; Bringezu F; Warriner H; Zasadzinski JA, More than a monolayer: Relating lung surfactant structure and mechanics to composition. Biophysical Journal 2004, 87 (6), 4188–4202. [PubMed: 15454404]
62. Takamoto DY; Lipp MM; von Nahmen A; Lee KY; Waring AJ; Zasadzinski JA, Interaction of lung surfactant proteins with anionic phospholipids. Biophys J 2001, 81 (1), 153–69. [PubMed: 11423403]
63. Alonso C; Waring A; Zasadzinski JA, Keeping lung surfactant where it belongs: protein regulation of two-dimensional viscosity. Biophys J 2005, 89 (1), 266–73. [PubMed: 15833995]
64. Lee KYC; Gopal A; von Nahmen A; Zasadzinski JA; Majewski J; Smith GS; Howes PB; Kjaer K, Influence of palmitic acid and hexadecanol on the phase transition temperature and molecular packing of dipalmitoylphosphatidyl-choline monolayers at the air-water interface. Journal of Chemical Physics 2002, 116 (2), 774–783.
65. Ding J; Warriner HE; Zasadzinski JA, Viscosity of two-dimensional suspensions. Phys Rev Lett 2002, 88 (16), 168102. [PubMed: 11955269]
66. Takamoto DY; Lipp MM; von Nahmen A; Lee KYC; Waring AJ; Zasadzinski JA, Interaction of lung surfactant proteins with anionic phospholipids. Biophysical Journal 2001, 81 (1), 153–169. [PubMed: 11423403]

67. vonNahmen A; Schenk M; Sieber M; Amrein M, The structure of a model pulmonary surfactant as revealed by scanning force microscopy. Biophysical Journal 1997, 72 (1), 463–469. [PubMed: 8994633]

68. Scarpelli EM; David E; Cordova M; Mautone AJ, Surface tension of therapeutic surfactants (exosurf neonatal, infasurf, and survanta) as evaluated by standard methods and criteria. American journal of perinatology 1992, 9 (5–6), 414–9. [PubMed: 1418146]

69. Chongsiriwatana NP; Patch JA; Czyzewski AM; Dohm MT; Ivankin A; Gidalevitz D; Zuckermann RN; Barron AE, Peptoids that mimic the structure, function, and mechanism of helical antimicrobial peptides. Proc Natl Acad Sci U S A 2008, 105 (8), 2794–9. [PubMed: 18287037]

70. Cabre EJ; Martinez-Calle M; Prieto M; Fedorov A; Olmeda B; Loura LMS; Perez-Gil J, Homo- and hetero-oligomerization of hydrophobic pulmonary surfactant proteins SP-B and SP-C in surfactant phospholipid membranes. J Biol Chem 2018, 293 (24), 9399–9411. [PubMed: 29700110]

71. Czyzewski AM; Jenssen H; Fjell CD; Waldbrook M; Chongsiriwatana NP; Yuen E; Hancock RE; Barron AE, In Vivo, In Vitro, and In Silico Characterization of Peptoids as Antimicrobial Agents. PLoS One 2016, 11 (2), e0135961. [PubMed: 26849681]

72. Seo J; Ren G; Liu H; Miao Z; Park M; Wang Y; Miller TM; Barron AE; Cheng Z, In vivo biodistribution and small animal PET of (64)Cu-labeled antimicrobial peptoids. Bioconjug Chem 2012, 23 (5), 1069–79. [PubMed: 22486390]

73. Madsen J; Panchal MH; Mackay RA; Echaide M; Koster G; Aquino G; Pelizzi N; Perez-Gil J; Salomone F; Clark HW; Postle AD, Metabolism of a synthetic compared with a natural therapeutic pulmonary surfactant in adult mice. J Lipid Res 2018, 59 (10), 1880–1892. [PubMed: 30108154]

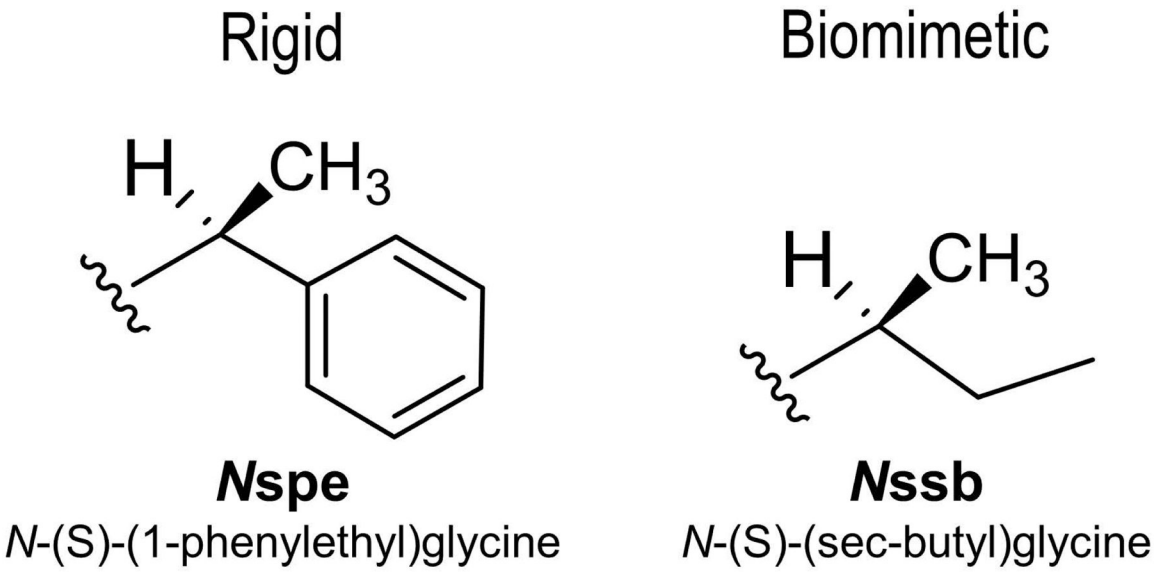

Figure 1:
Comparison of peptoid monomer side chain structures (rigid versus biomimetic).

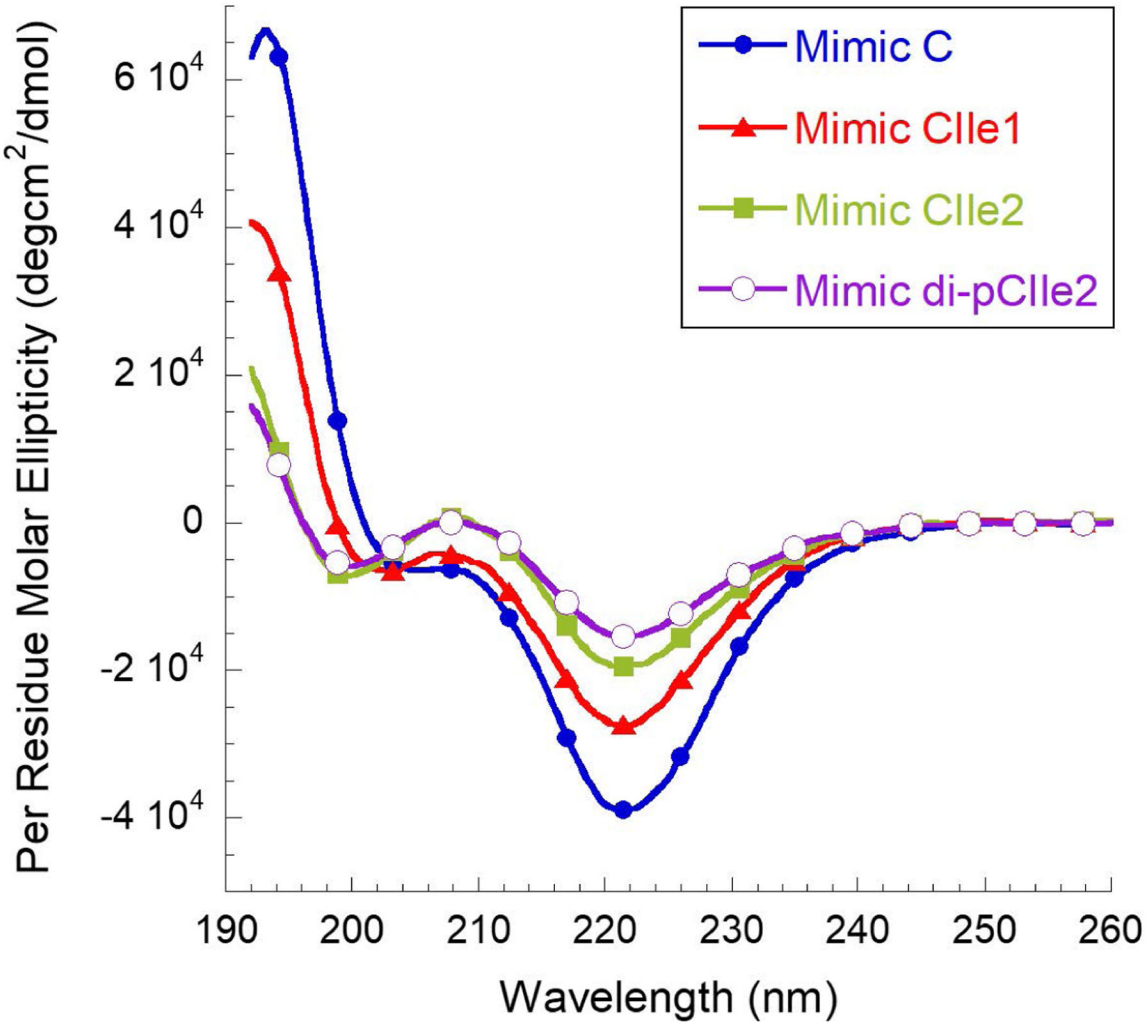

Figure 2:

Circular dichroism (CD) spectra of the peptoid-based SP-C mimics (Mimics C, CIle1, CIle2, and di-pCIle2) showing qualitatively similar characteristics of peptoid helices. As the aliphatic content is increased, the CD spectra display features that are progressively similar to a polyproline type I peptide helix. Spectra were acquired in methanol at a concentration of ~ 60 μM at room temperature.

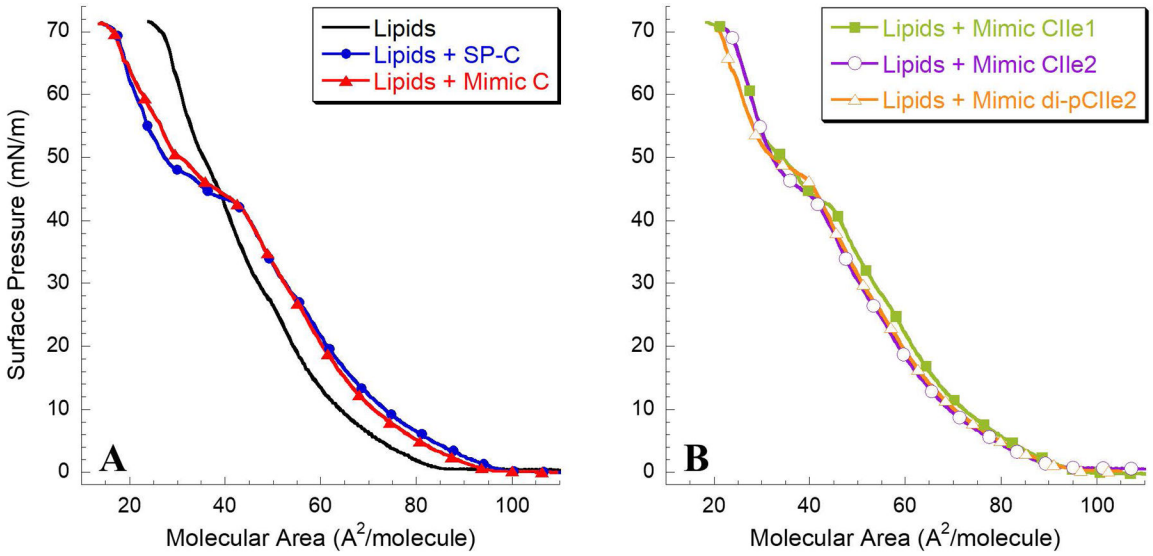

Figure 3:

Langmuir-Wilhelmy surface balance (LWSB) studies at 37°C. (A) Surface pressure-area isotherms obtained for DPPC:POPG:PA (68:22:9, by weight) alone, with 1.6 mol% SP-C, and with 1.6 mol% Mimic C; (B) Lipids with 1.6 mol% Mimic CIle1, Mimic CIle2, and Mimic di-pCIle2. Isotherms were collected on a buffered subphase (150 mM NaCl, 10 mM HEPES, 5 mM CaCl2, pH 6.90).

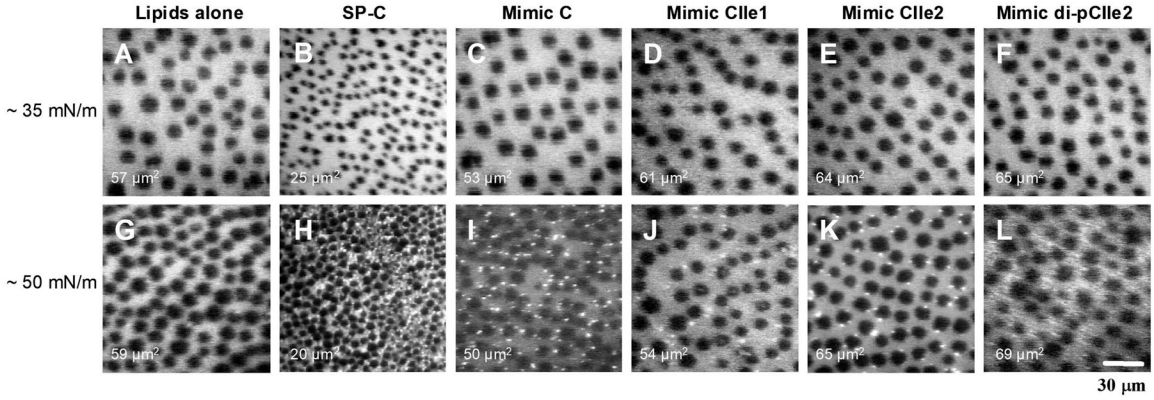

Figure 4:

Fluorescence microscopy (FM) micrographs at 37°C corresponding to a surface pressure of ~ 35 mN/m and ~ 50 mN/m for DPPC:POPG:PA (68:22:9, by weight) alone (panels A and G), with 1.6 mol% SP-C (panels B and H), Mimic C (panels C and I), Mimic CIle (panels D and J), Mimic CIle2 (panels E and K), and Mimic di-pCIle2 (panels F and L). Average size of the dark LC domains for each film is indicated in the lower left of each panel.

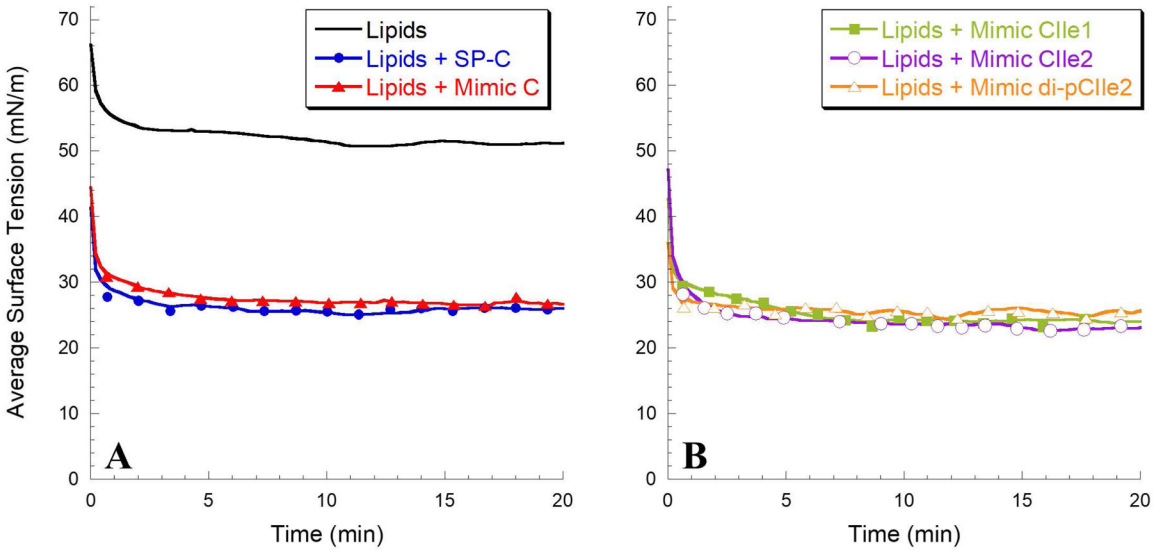

Figure 5:

Static pulsating bubble surfactometry (PBS) results displaying surface tension as a function of time. (A) Lipid mixture alone and with 1.6 mol% SP-C and Mimic C; (B) Lipid mixture with 1.6 mol% Mimics CIle1, CIle2, and di-pCIle2. Measurements were taken at a bulk surfactant concentration of 1 mg/mL lipids and at 37°C.

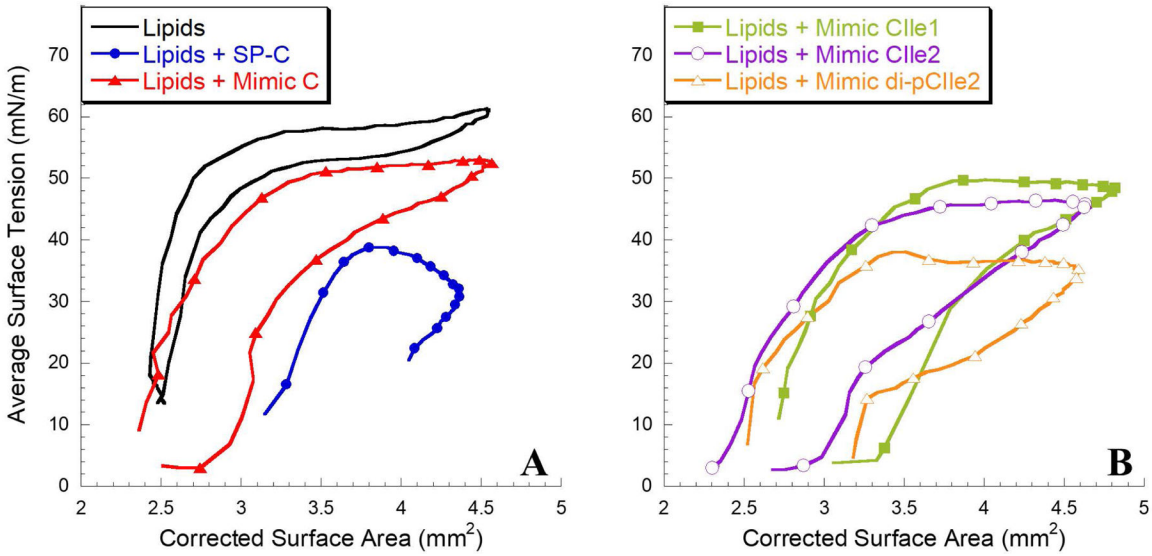

Figure 6:

Dynamic pulsating bubble surfactometry (PBS) results displaying surface tension as a function of surface area at an oscillation frequency of 20 cycles/min, after 5 minutes of initial cycling. (A) Lipid mixture alone and with 1.6 mol% SP-C and Mimic C. (B) Lipid mixtures with 1.6 mol% Mimics CIle1, CIle2, and di-pCIle2. Measurements were taken at a bulk surfactant concentration of 1 mg/mL lipids and at 37°C. Loop directions are clockwise with expansion followed by compression. A one-way analysis of variance with post hoc Tukey-Kramer multiple comparison testing was used to analyze maximum surface tension results. All groups were significantly different ($p < 0.05$) from each other except for Lipids + SP-C and Lipids + Mimic di-pCIle2.

Table 1:

Elements of Surface Activity

Key Aspect of Surface Activity	Technique	Ideal Features of Mimic
Monolayer-phase behavior and lipid respreading	LWSB	(i) Early lift-off (> 100 $Å^2$/molecule) (ii) Biomimetic plateau region between 40–55 mN/m (iii) High maximum surface pressure near 72 mN/m (iv) No significant hysteresis between successive surface area compressions
Surface film morphology as a function of surface pressure	FM	(i) LC domain size ~ 25 μm^2 (ii) Bright film domains appear upon film compression
Rapid adsorption to air-water interface	Static PBS	Reach surface tension <25 mN/m in <1 min
Reduce and control surface tension as a function of surface area	Dynamic PBS	(i) Low (near zero) minimum surface tension with minimal compression (low compressibility) (ii) Low maximum surface tension (iii) No significant hysteresis between successive compression-expansion loops

Table 2:

Structure of Peptoid-Based SP-C analogues

Compound	Structure
Mimic C H-*N*pm*N*pm*N*Pro*N*Val*N*pm*N*Leu*N*Lys*N*Lys(*N*spe)$_{14}$-NH$_2$ 3279 g/mol	Hydrophobic, helical region 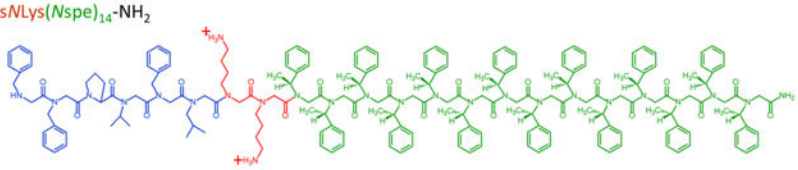
Mimic CIle1 H-*N*pm*N*pm*N*Pro*N*Val*N*pm*N*Leu*N*Lys*N*Lys(*N*spe*N*spe*N*ssb)$_4$*N*spe*N*spe-NH$_2$ 3087 g/mol	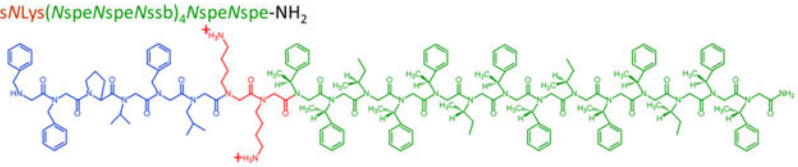
Mimic CIle2 H-*N*pm*N*pm*N*Pro*N*Val*N*pm*N*Leu*N*Lys*N*Lys*N*ssb(*N*spe*N*ssb*N*ssb)$_4$*N*spe-NH$_2$ 2847 g/mol	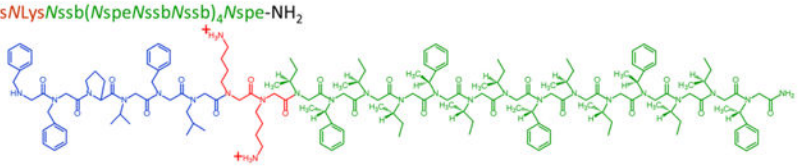
Mimic di-pCIle2 H-*N*ocd*N*ocd*N*Pro*N*Val*N*pm*N*Leu*N*Lys*N*Lys*N*ssb(*N*spe*N*ssb*N*ssb)$_4$*N*spe-NH$_2$ 3240 g/mol	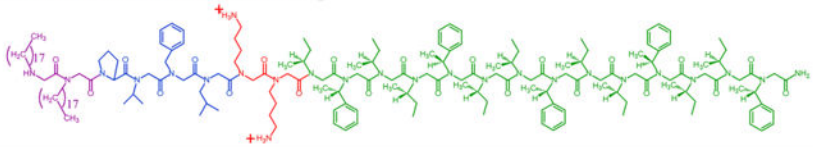

Green represents the hydrophobic helical region, red the lysine-like side chains, purple the C-18 alkyl chains (*N*ocd) that mimic the palmitoyl chains of natural SP-C, and blue the N-terminal region.